

## CHAPTER III RESULTS AND DISCUSSION



### 3.1 MCM-41 Synthesis

Silica MCM-41 is a member of M41S family with a hexagonal array of two-dimension pores. By using cetyltrimethyl ammonium bromide (CTAB) as a template for the synthesis of mesoporous silica, MCM-41, via liquid crystal templating mechanism (LCT) the pore will mimic the surfactant liquid crystal structure. General procedure for synthesizing MCM-41 using  $\text{SiO}_2$  as the precursor, needs to use high temperature and long reaction time in autoclave [3-4,8,37,42]. Although alkoxide precursor, such as TEOS or TMOS, is often used to reduce reaction temperature and time, these precursors are expensive compared with  $\text{SiO}_2$ . Recently, Haskouri synthesized MCM-41 from silatrane precursor prepared from expensive starting materials via a complicated route [7,19,40], giving good quality MCM-41 with surface area of  $1130 \text{ m}^2\text{g}^{-1}$  [19]. Wongkasemjit's method using an inexpensively starting material  $\text{SiO}_2$ , as precursor, results in high purity of the silatrane product in one step. The result shows that silatrane from our method is successfully used to synthesize high quality MCM-41 having remarkable surface area up to  $2,400 \text{ m}^2/\text{g}$  using lower and shorter reaction temperature and time, respectively.

### 3.2 Effect of Ion Concentration

Ion concentration is one of the important parameter in micelle formation. Changing ion concentration will effect to the size and structure of liquid crystal, as stated by Huo et al. (1994b) and Firouzi et al. (1995). To compare Haskouri's result, the following condition, Si:0.3CTAB:yNaOH:3.5TEA:90H<sub>2</sub>O at ambient temperature was used; where y was varied in the range of 0.15-1.0. As shown in fig.3.1, XRD spectra give only hk0 reflections and no reflections at diffraction angle larger than 6 degree 2 $\theta$  was observed. The positions of these peaks approximately fit the position for the hk0

reflections from a hexagonal unit cell with  $a=b$  and  $c=\infty$ . From the result, only the NaOH ratios of 0.25 and 0.35 showed a clear pattern of MCM-41 by showing 3 peak positions belonging to 100, 110 and 200 reflections of long range structural ordering.

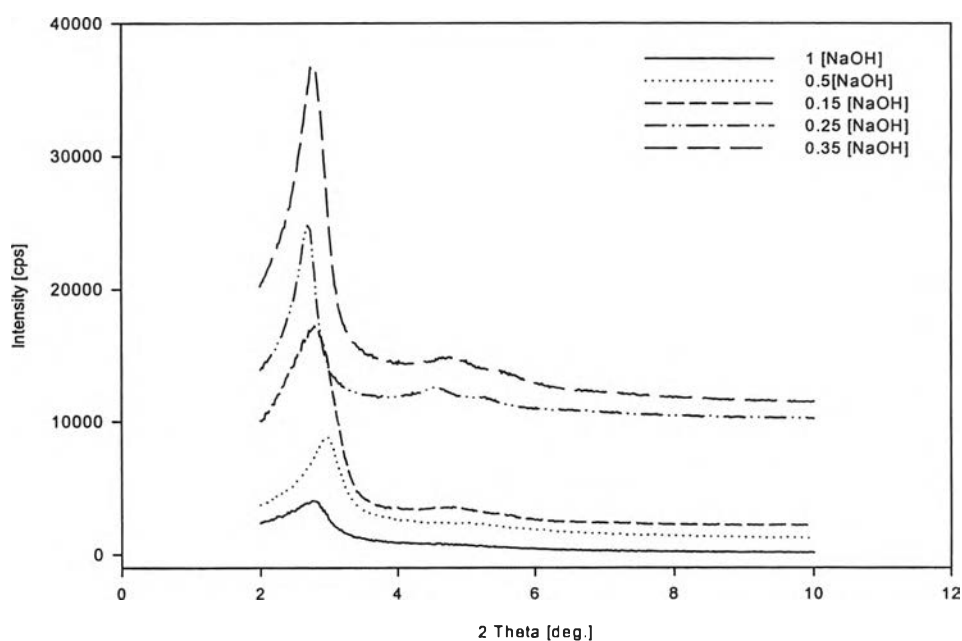


Figure 3.1 XRD spectrum of synthesized MCM-41 at different ion concentration.

For the others, only the first single peak was observed. The results indeed showed the effect of ion on liquid crystal formation. Too high NaOH concentration resulted in a decrease in the XRD peak intensity. Generally, addition of electrolyte causes a decrease in electrical repulsion between ionic head group due to the decrease in the thickness of the ionic atmosphere around the ionic head group, thus decreased CMC. However, at high ion concentration charge repulsion occurred, inhibiting the hexagonal array to form. For BET results, the surface area of the 0.25 NaOH ratio is higher and the pore size is smaller than those of the 0.35 ratio, as shown in table 3.1. That means, the liquid crystal of the 0.25 ratio is more compact than that of the 0.35 ratio.

Table 3.1 The BET analysis of MCM-41 synthesized at 60°C at different NaOH ratio

NaOH ratio	BET Surface Area (m <sup>2</sup> /g)	Pore volume (cc/g)	Average Pore size (Å)
0.25	1850	1.015	22
0.35	1100	0.711	25

### 3.3 Effect of Temperature

Temperature is also a factor affecting to the liquid crystal formation [12-13,23,43]. In this study, the ratio of 0.25 NaOH giving the highest surface area was used. When increasing the mixing temperature from 40° to 100°C at the formula ratio of Si:0.3CTAB:0.25NaOH:3.5TEA:90H<sub>2</sub>O, the XRD spectra showed the sharper peak with a little shift of peaks to the lower degree two theta, as shown in fig.3.2.

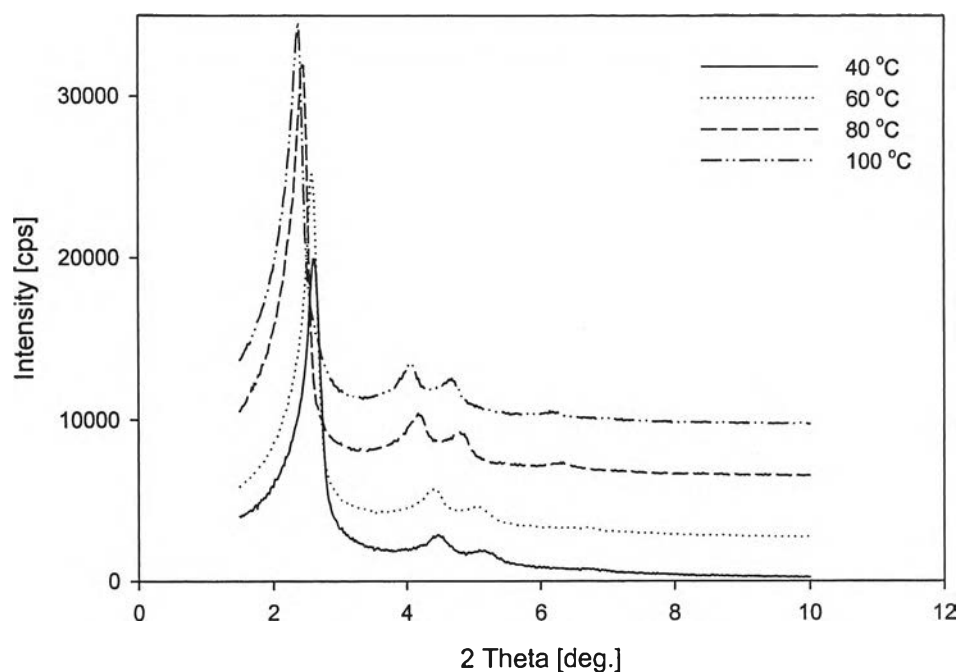


Figure 3.2 XRD spectrum of synthesized MCM-41 at different temperature.

It may refer to the bigger pore sizes and more perfect alignment of hexagonal mesoporous. The reason for the bigger pore may come from the fact that the higher temperature makes the surfactant tail more flexible to move or vibrate more freely, causing more occupied space of surfactant in the pore, as a result, causing a bigger pore after removed. The further explanations are given in previous works, e.g. Zhou *et al*, reported that the mechanism of channel growth is relied on interaction between silicate anion and surfactant. His study using HRTEM (High Resolution Transmission Electron Microscope) showed that this process was diffusion controlled. At high temperature the entire process faster resulted in uniform channel diameter and gave maximum diameter of the surfactant rod. However, in our work when increasing temperature up to 60°C, the XRD spectrum showed clearly pattern of MCM-41. The 110 and 200 reflections are distinguishably separated, caused from long range ordering of hexagonal array. For confirmation, TEM image was studied. The TEM image of MCM-41 at 60°C shown in

Fig 3.3 shows the TEM results which two directions of image were corrected. Fig 3.3a shows the hexagonal arrangement corresponding to the straight channels of MCM-41 along the channel direction or the incident beam is along the 001 direction. Fig. 3.3b is the TEM image in the perpendicular direction, which the channel is assumed to be cylindrical. In principle, the pore diameter is calculated from the perpendicular direction due to the image projected along the incident beam, which may give somewhat less than actual value.

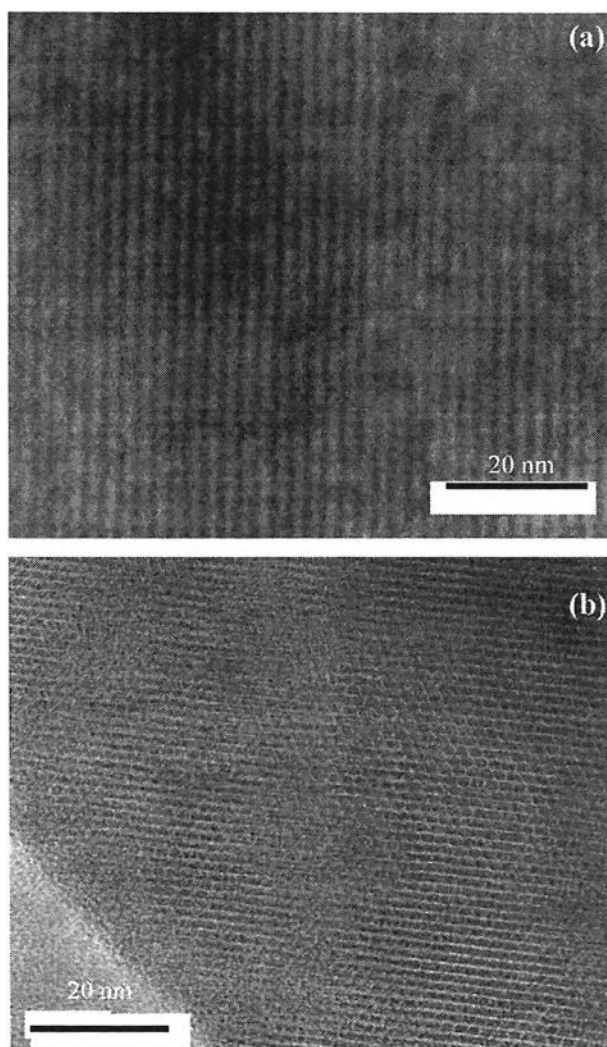


Figure 3.3 TEM image of hexagonal arrangement, MCM-41, at 60°C (a) along the channel (b) perpendicular the channel.

The TEM results in fig.3.4 show the bigger pore sizes when increased the temperature, which is in agreement with the XRD results.

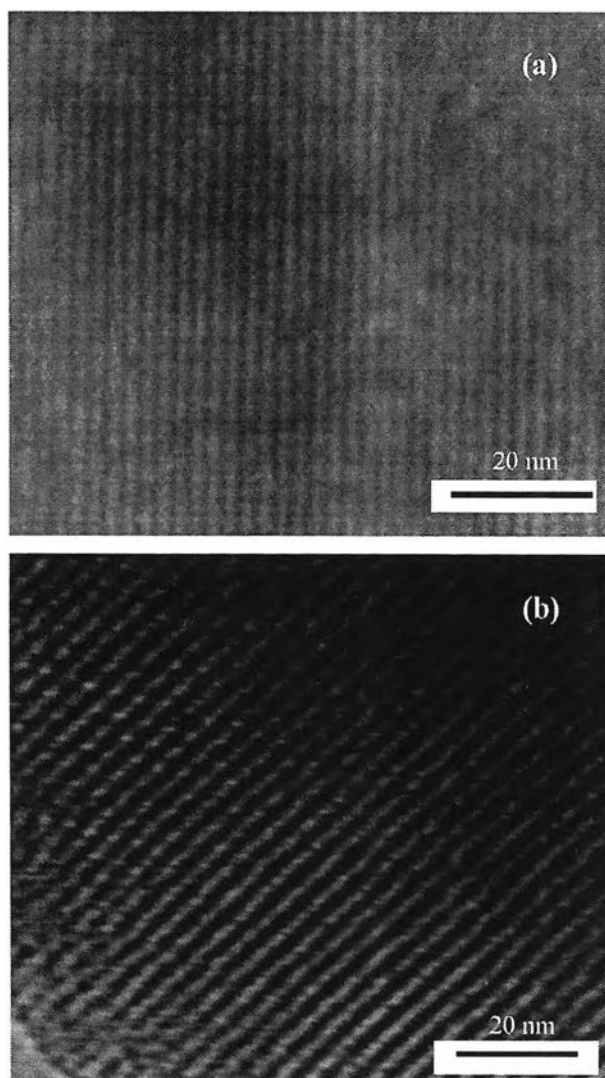


Figure 3.4 Effect of temperature on TEM image of MCM-41 at (a) 60° and (b) 100°C.

The diameters of the channel calculated from fig.3.4a and 3.4b are 23.5 and 31.3 Å, respectively. Channel diameter from sorption measurements using BJH (Barrett, Joyner and Halenda) formula showed the same results as XRD and TEM. The average pore diameters of MCM-41 at higher temperature are also larger than those of lower

temperature. The diameter at 60° and 100°C are 22 and 35 Å, respectively. This size is close to that of CTABr micelle, 39.7 Å. From the study of Cheng *et al*, the channel diameter of MCM-41 in his work using the sorption technique as our work showed the increase in channel diameter from 27.1 to 36.5 Å when increasing temperature from 70° to 165°C for the reaction time of 48 hr. This reaction time is 16 times longer than the reaction time used in our study while the diameter is quite comparable under higher temperature. In addition, it was reported that pore size and uniformity of product prepared under identical condition but various silicate anion are not the same. This consequence results from the different diffusion rate of silicate anion from different source of silica. In this case, our precursor, silatrane, is easily formed silicate anion under basic condition so it may diffuse faster and undergo condensation faster. In fact, there are two ways to synthesize larger pore MCM-41 materials in literature, which are the uses of long chain surfactants and a swelling agent. However, there are many drawbacks. Long chain surfactants are not available and very expensive. The swelling agent expands the pore size product but decreases the quality of product. Recently, pore-size enlargement of MCM-41 is observed through a hydrothermal treatment in the mother liquor or post synthesis hydrothermal treatment.

As a result, surface area and pore volume of MCM-41 obtained from silatrane synthesized by the OOPS method are impressively high and much higher than atrane synthesized from a nother route probably due to a purer silatrane product obtained, as shown in table 3.2.

Table 3.2 The BET analysis of MCM-41 synthesized at different temperature

Temperature (°C)	BET Surface Area (m <sup>2</sup> /g)	Pore Volume (cc/g)	Average Pore Size (Å)
40	2050	1.060	21
60	2098	1.188	22
80	1630	1.333	33
100	1550	1.080	35

From the study of Haskouri *et al.*, it involved in the synthesis of mesoporous material using atrane prepared by other route [7,40], as precursor. In their work many types of mesoporous material were obtained including MCM-41. The surface area of MCM-41 prepared from the same condition between their work and ours is significantly different. They obtained the highest surface area of 1130 m<sup>2</sup>/g whereas ours gave approximately twice higher, 2098 m<sup>2</sup>/g. The reason may again come from the purity of the silatrane precursor prepared using Wongkasemjit's synthetic method giving higher purity and more homogeneous, as indicated by one sharp mass loss transition of TGA of silatrane and high intensity of XRD spectrum of MCM-41.

### 3.4 Effect of Aging Time

In this study, since alkoxide precursor is used and MCM-41 is synthesized via sol-gel process, involving in hydrolysis and condensation reactions it should take a period of time to become equilibrium. However, no induction period is found in the course of MCM-41 synthesis because it has been claimed that the synthesis depends on source of silicate and surfactant used [35]. Aging time represents the time between the formation of gel and the removal of solvent. For alkoxide-derived gel, condensation between surface functional groups continues to occur after gel point. During aging, there are changes in most texture and physical properties of the gel. The strength of the gel thereby increases with aging, meaning that aging time is one of the parameter that needs to be considered. In this case, hydrolysis and condensation of silatrane gave Si-O-Si linkage, as shown below.

#### Hydrolysis:



#### Condensation:



By fixing the formula ratio of Si:0.3CTAB:0.25NaOH:3.5TEA:90H<sub>2</sub>O at the mixing temperature of 60°C, aging time was varied from 1 to 12 hr. The XRD result is shown in Fig.3.5. The XRD spectra do not significantly show any difference for all aging time, as indicated in previous works. However, the reaction time used is much lower than other works using either SiO<sub>2</sub> or TEOS or TMOS.

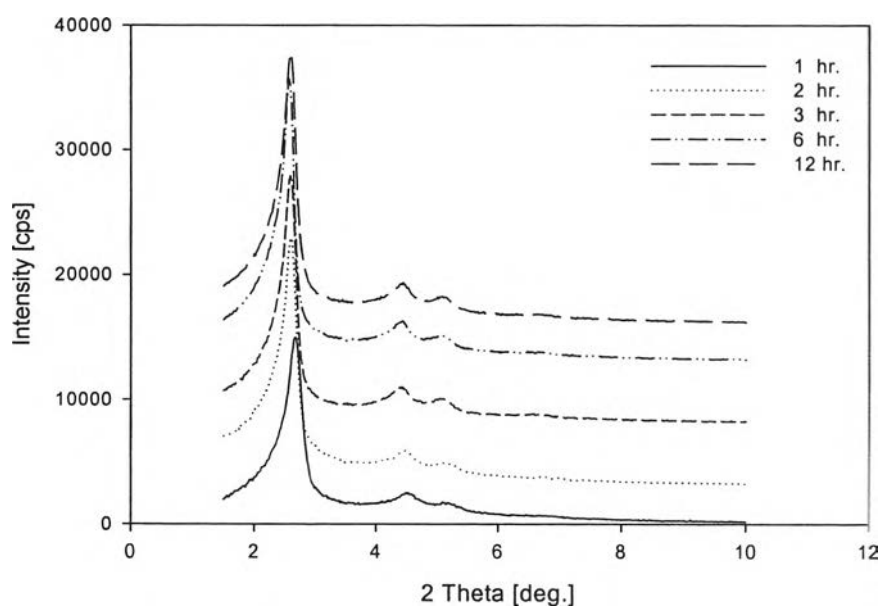


Figure 3.5 Effect of aging time on XRD spectrum of MCM-41 synthesized at 60°C.

BET surface area, pore size and pore volume are shown in Table 3.3. It was found that the aging time also gave no effect on the surface area or pore volume, as coincided with the XRD results.

Table 3.3 The BET analysis of MCM-41 synthesized at different aging time

Aging Time (hr)	BET Surface Area (m <sup>2</sup> /g)	Pore Volume (cc/g)	Average Pore Size (Å)
1	1812	1.101	24
2	2054	1.188	22
3	2098	1.015	22
6	2044	1.165	23
12	2085	1.153	22

### 3.5 Effect of Surfactant Concentration

This study used the formula ratio of Si:yCTAB:0.25NaOH:3.5TEA:90H<sub>2</sub>O where y was in the range of 0.2 to 0.6 at the mixing temperature of 60°C. At the surfactant ratio of 0.2, XRD spectrum showed broader peak and a little bit lower intensity when compared with the others, see Fig.3.6, while other ratios showed no difference. The reason may be explained by Cheng's work. He proposed the mechanism for surfactant micelle catalyst, which relies on electrostatic interaction at the micelle-silicate interface. The Br<sup>-</sup> and OH<sup>-</sup> exchange in surfactant accelerates the hydrolysis and condensation of organosilicate. The increasing exchange will increase the basicity of the micelle surface, promoting both the hydrolysis and condensation. Thus, low surfactant ratio may not be enough to give high quality of MCM-41. The BET surface area results are shown in Table 3.4.

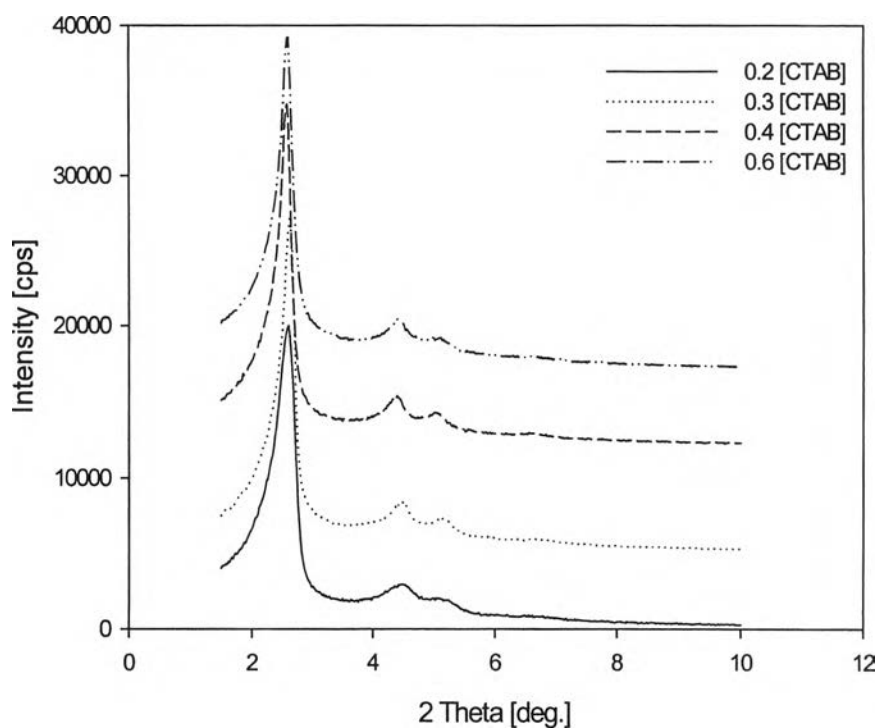


Figure 3.6 Effect of surfactant concentration on XRD spectrum of MCM-41 synthesized at 60°C.

Table 3.4 The BET analysis of MCM-41 synthesized at different surfactant ratio and two different temperatures

Surfactant ratio	BET Surface Area (m <sup>2</sup> /g)	Pore Volume (cc/g)	Average Pore Size (Å)
<b>60°C</b>			
0.2	1952	1.047	21
0.3	2098	1.188	22
0.4	2278	1.311	23
0.6	2430	1.288	22
<b>100°C</b>			
0.3	1550	1.080	35
0.4	1900	1.560	34
0.6	2100	1.723	33

The results show that the increasing surfactant ratio affected only the surface area. That means, the micelle size was still the same even the surfactant concentration increased. The higher surfactant ratio, the longer of micelle rod resulted in the higher surface area. The highest surface area obtained is as high as 2,430 m<sup>2</sup>/g. At reaction temperature of 100°C, the surface area decreased while the pore volume much increased. This is corresponding to the thermal expansion of micelle, which increases volume of liquid crystal. At the surfactant ratio of 0.6, surface area is extremely high, 2,100 m<sup>2</sup>/g and the pore volume is also as high as 1.723 cc/g. The average pore sizes are bigger for the mixing temperature of 100°C, as predicted.

The TEM images of MCM-41 obtained using the surfactant ratio of 0.6 are shown in Fig.3.7. The pore structure also showed the hexagonal array, as can be seen in Fig 3.7a. In addition, increasing temperature from 60° to 100°C also showed the same trend as those shown in Fig.3.2. The XRD peak is sharper and shift to the lower degree two theta when temperature is increased, as shown in Fig.3.8, referring to the bigger pore sizes. In addition, Fig 3.8b shows the peak of 210 reflection which refers to better quality of MCM-41. The better quality is caused from the enhancement of high diffusion of silicate anion at high temperature and the catalytic effect of higher surfactant ratio.

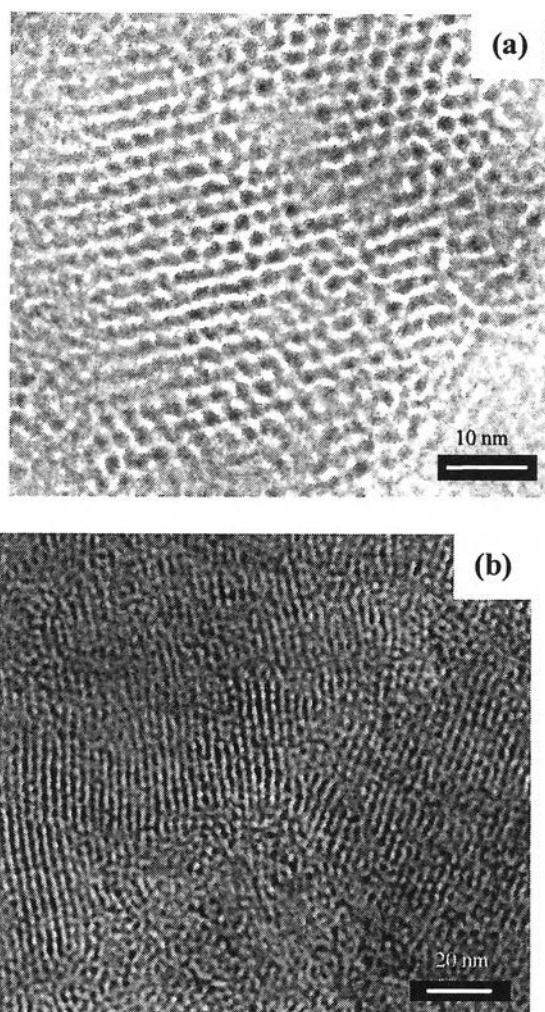


Figure 3.7 TEM images of the hexagonal arrangement of MCM-41 at the surfactant ratio of 0.6.

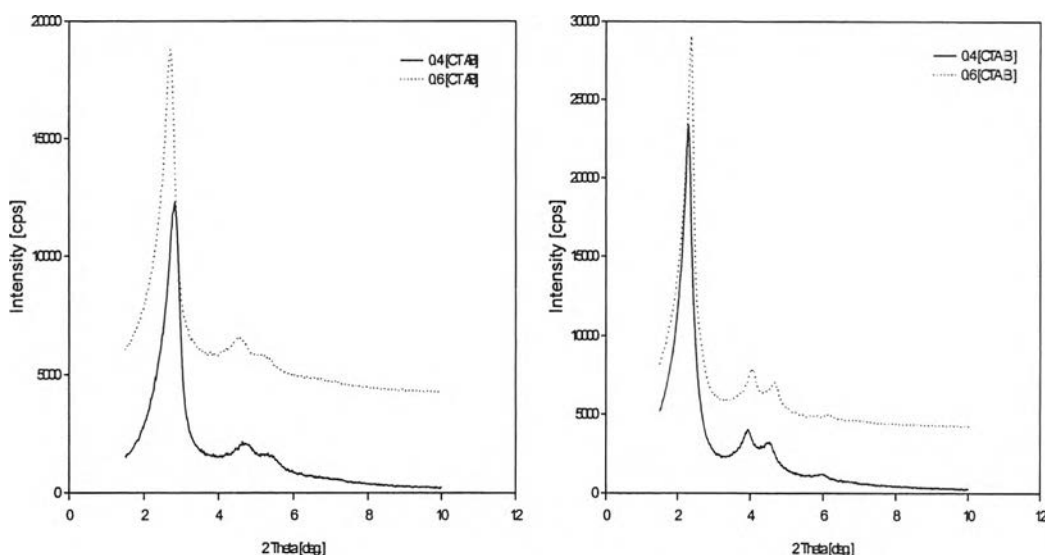


Figure 3.8 Effect of temperature on XRD spectrum of MCM-41 at the surfactant ratio of 0.6 and different mixing temperature of (a) 60° and (b) 100°C.

### 3.6 V-MCM-41 Synthesis

MCM-41 supported vanadium samples (V loading ranging from 0.5 to 25 wt %) give well-defined XRD patterns corresponding to MCM-41 structures, as shown in Fig 3.9. The better resolution of (110), (200), (210) and (300) peaks indicates the achievement of particularly high crystallinity. Expectedly, the XRD resolution shifted to higher 2Theta with increasing vanadium content, probably referring to smaller pore size. It may be caused from vanadium incorporated inside the framework making the wall thickness increase, resulting in a decrease in pore size.

It is well known that vanadium supported on siliceous material can be easily hydrated, changing the nature of V species from tetracoordinated V to penta- or hexacoordinated sites [1,30,33]. For this reason, and in order to determine the exact vanadium environment, diffusive reflectance spectroscopy in the UV-Vis region of MCM-41-supported samples was conducted.

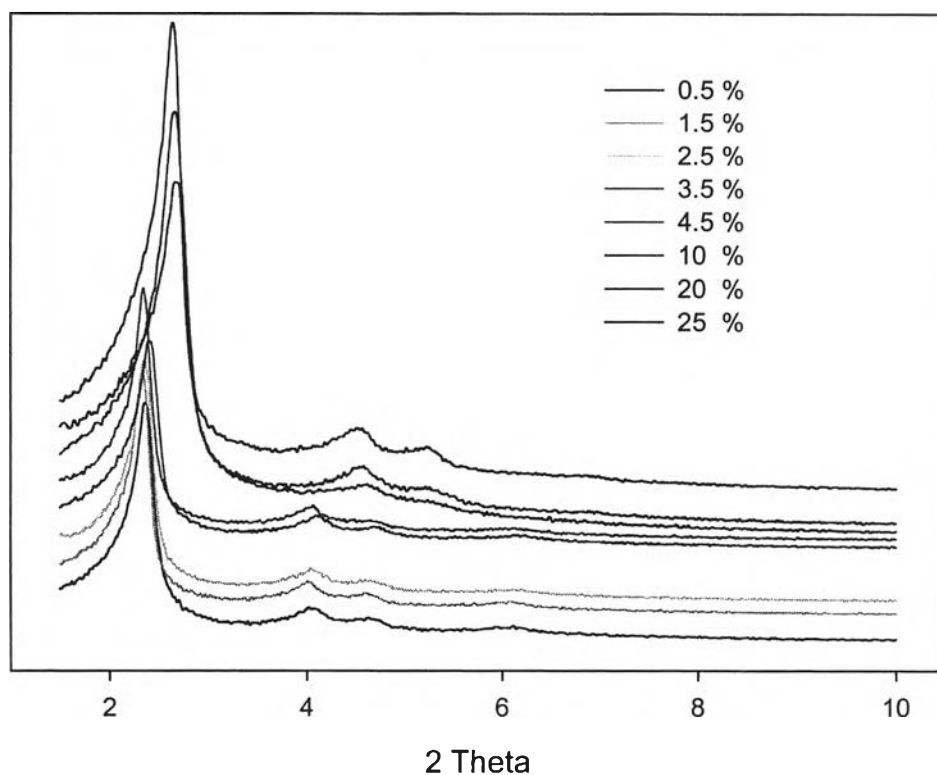


Figure 3.9 X-ray diffraction patterns of V-MCM-41 catalysts having V content of: (a) 0.5%, (b) 1.5%, (c) 2.5%, (d) 3.5%, (e) 4.5%, (f) 10%, (g) 20% and (h) 25%.

All V-MCM-41 samples show strong UV-vis absorption bands with overlapping maxima around 274 and 380 nm, as shown in Fig.3.10. The 274 nm band seems to have a relatively higher intensity for higher vanadium loading. These bands are assigned to a low-energy charge transfer transitions between tetrahedral oxygen ligands and a central  $V^{5+}$  ion. Typically, a tetrahedral environment is found for framework  $V^{5+}$  ions in zeolites and also for some supported  $V_2O_5$  catalysts. Kevan and co-worker [1] suggested that UV band at 274 nm observed for V-MCM-41 corresponded to the vanadium incorporated inside the framework of MCM-41. Since the vanadium source added to the synthesized gel is a  $V^{4+}$  salt, the UV-vis results clearly indicate that most of the  $V^{4+}$  ions are oxidized to  $V^{5+}$  ions during synthesis. The 380 nm band can be assigned to pseudo-octahedrally coordinated  $V^{5+}$  species as a consequence of the interaction of tetrahedral sites with two molecules of water [30]. In the visible region no additional absorption bands was

observed, especially near 600 nm, corresponding to d-d transitions of vanadyl  $\text{VO}^{2+}$  ions. Since the d-d transitions of vanadyl  $\text{VO}^{2+}$  ions are generally 10-30 times weaker than those of charge transfer transitions, such absorption is apparently undetected by diffuse reflectance UV-vis. Baltes [41] illustrated that a ligand in the sixth position on the vanadium ion axial to the  $\text{V} = \text{O}$  bond altered from the vanadyl oxygen bond. This effect can be estimated from the energy difference between the first and second d-d transitions ( $\Delta$ ) since the first band is red-shifted and the second band is blue-shifted. The higher  $\Delta$ , the more pronounced effect of the coordination of the sixth ligand to the  $\text{VO}^{2+}$  cation. It can be concluded that the  $\text{V}[\text{H}_2\text{O}]_4[\text{OH}]_2$  complexes were deposited on  $\text{SiO}_2$  by the MDD method [28], that is a promising way to develop highly dispersed transition metal oxides on supports, showing a clear axial coordination by the ligand number six coordinated with most probably an oxygen atom or hydroxy group of the support.

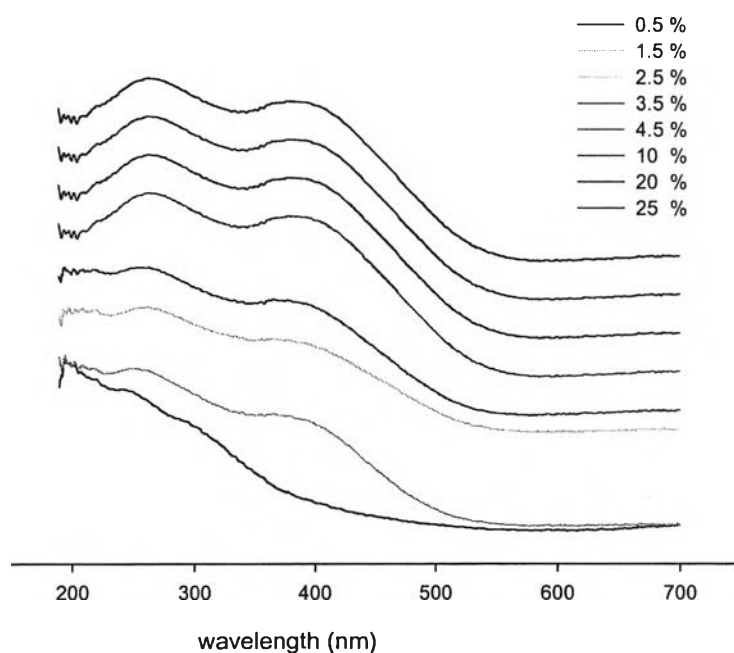


Figure 3.10 Diffuse reflectance UV-vis spectra of VMCM-41 at different vanadium concentration of (a) 0.5%, (b) 1.5%, (c) 2.5%, (d) 3.5% (e) 4.5%, (f) 10% (g) 20% and (h) 25%.

Upon calcination in air atmosphere, the V-MCM-41 samples were changed from green to white due to the oxidation state change of  $\text{VO}^{2+}$  to  $\text{V}^{5+}$  ions [11,15]. After exposure of these calcined samples to hydrated air the color rapidly changed to bright yellow followed by orange. This indicates additional coordination of water molecules to the  $\text{V}^{5+}$  ions [11,26,28,32], as reflected by the broadening of the UV-vis spectrum toward lower energy.

Temperature-programmed reduction (TPR) was carried out to investigate the oxidation states of different loading of vanadium oxide deposited on the activated silica support and to relate these oxidation states with activity studies of the catalysts. TPR profiles of various amounts of vanadia-loaded are illustrated in Fig. 3.11.

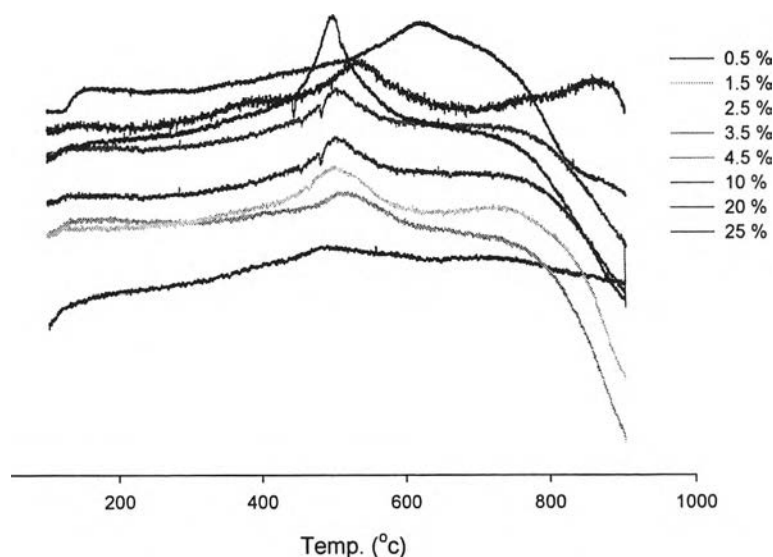


Figure 3.11  $\text{H}_2$ -TPR of V-MCM-41 at different vanadium concentration of (a) 0.5%, (a) 1.5%, (c) 2.5%, (d) 3.5%, (e) 4.5%, (f) 10%, (g) 20%, and (h) 25%.

It should be noted that the morphological properties of support materials (e.g. surface area, porosity) and the level of impurities (foreign compounds) as well as the method of preparation of vanadia may play an important role in determining the

reducibility of vanadia. In addition the reduction temperature is also dependent on the reduction condition, such as,  $H_2$  partial pressure and heating rate. As shown in Fig. 3.11, there was only a single reduction temperature peak observed in the range of 500-525 °C for V-MCM-41 with vanadium content between 0.5 to 10 wt%, demonstrating the formation of an oxide in which vanadium has an oxidation state between  $V^{5+}$  and  $V^{4+}$ . This suggests that the temperature reduction peak in the TPR profile should be assigned to surface species, which is due to the subsistence of monomeric surface vanadia on silica support. Reddy and co-worker [15] reported the peak at 500°C corresponding to the reduction temperature of  $V^{5+}$  ( $V^{5+}$  to  $V^{4+}$ ). Wachs and co-worker [33] reported that the reduction peak for surface vanadium oxide species highly dispersed on a silica support appeared at ca. 525 °C. The TPR results reported in Fig. 3.11 thus indicate that vanadium is mainly present as a  $V^{5+}$  species, in agreement with the UV-visible results. In the samples with 20 and 25 wt% vanadium content, the reduction temperatures were shifted to 570 and 620 °C, respectively. The peak at 570C should be related to the reduction of dispersed tetrahedral vanadium species, while the peak at 620 C should be corresponding to the reduction of polymeric  $V^{5+}$  species, as  $V_2O_5$ -like [1,6,10,27,30]. The progressive shift of the maximum TCD signal to high temperature with the vanadium loading could be related to a progressive formation of high polymeric vanadium species.